A major purpose of the Technical Information Center is to provide the broadest dissemination possible of information contained in DOE's Research and Development Reports to business, industry, the academic community, and federal, state and local governments.

Although a small portion of this report is not reproducible, it is being made available to expedite the availability of information on the research discussed herein.

LA-UR -86-4339

CONF-861207--15

LA-UR--86-4339

DE87 003755

TITLE ANALYSIS OF PICOSECOND PULSED LASER MELTED GRAPHITE

AUTHOR(S) J. Steinbeck, G. Braunstein, J. Speck, M. S. Dresselhaus, C. Y. Huang, A. M. Malvezzi, and N. Bloembergen

SUBMITTED TO Proceedings of the Symposium on Beam-Solid Interactions, Boston, MA, December 1-6, 1986

DISCLAIMER

Los Alamos Los Alamos National Laboratory
Los Alamos, New Mexico 87545

FORM NO 836 R4
ST NO 2629 5-81

ANALYSIS OF PICOSECOND PULSED LASER MELTED GRAPHITE

J. Steinbeck*, G. Braunstein*, J. Speck*, M.S. Dresselhaus*, C.Y. Huang**, A.M. Malvezzi***, N. Bloembergen***
*Massachusetts Institute of Technology, Cambridge, MA 02139
**Los Alamos National Laboratory, Los Alamos, NM 87545
***Harvard University, Cambridge, MA 02138

Abstract

A Raman microprobe and high resolution TEM have been used to analyze the resolidified region of liquid carbon generated by picosecond pulse laser radiation. From the relative intensities of the zone center Raman–allowed mode for graphite at 1582cm^{-1} and the disorder–induced mode at 1360cm^{-1}, the average graphite crystallite size in the resolidified region is determined as a function of position. By comparison with Rutherford backscattering spectra and Raman spectra from nanosecond pulsed laser melting experiments, the disorder depth for picosecond pulsed laser melted graphite is determined as a function of irradiating energy density. Comparisons of TEM micrographs for nanosecond and picosecond pulsed laser melting experiments show that the structure of the laser disordered regions in graphite are similar and exhibit similar behavior with increasing laser pulse fluence.

Introduction

Currently, the primary focus of pulsed laser irradiation studies is the interaction of a high power laser pulse with a crystal lattice. The pulsed laser heating technique can also be applied to the study of high temperature materials and their phase transformations. Studies of the effects of pulsed laser irradiation on carbon have been undertaken to determine the high temperature properties of graphite and liquid carbon [2,3]. From these studies different conclusions about the properties of liquid carbon have been drawn.

A possible cause for the controversy might be that graphite enters different phases depending upon the duration and power density of the heating laser pulse. Transitions to different phases could then result from differences in the pressure applied to the surface induced by vaporisation. A phase diagram proposed by Ferraz and March[4] incorporating two liquid phases is given in Fig.. The metallic liquid phase was observed by Bundy[5] during pulsed current heating of graphite rods at high pressure. Transient electrical conductivity measurements at low pressure by Jones[6] indicated the insulating liquid phase. The phase transition between the insulating and metallic liquid phases has not been observed experimentally, but the transition must be first order to account for the radically different properties of the metallic and insulating liquid phases[4]. The existence of two separate liquid phases of carbon might then explain the conflicting measurements of the optical and thermal properties of liquid carbon and determine whether liquid carbon has both a liquid metal phase[2,7] and a liquid semiconductor or insulator phase[3,8].

Experimental Results

Raman microscopy and TEM have been used to study the structural properties of the disordered region remaining after graphite is irradiated with 20psec Nd:YAG laser pulses at .532μm. The results have been compared with the results from similar measurements on the disordered region remaining after irradiation with 30nsec ruby

laser pulses at 694nm[9,10]. In addition, the disorder layer thickness is calibrated for graphite irradiated by the 20psec pulses by comparisons of Raman spectra and Rutherford backscattering data of pulsed ruby laser irradiated graphite[1].

The results of Raman measurements in both the picosecond and nanosecond regime are given in Fig. 2 as a function of the irradiating energy density. Specifically, the intensity of the disorder–induced mode, I_{1360}, in graphite is compared to the intensity of the Raman–active mode, I_{1582}. The abscissas in the figure have been set so that comparisons between the two irradiating conditions can be made easily. The ratio of the intensities, I_{1360}/I_{1582}, has been related to the average crystallite size in disordered graphite by Tuinstra and Koenig[11] and is given on the right hand ordinate. As can be seen from Fig. 2, the general trend in both the nanosecond and picosecond regimes is to create a highly disordered region at irradiating energy densities close to the melt threshold. As the irradiating energy density is increased further the average crystallite size reaches a minimum and then begins to increase. It should be noted that the Raman spectra for picosecond pulses between 0.7 and 0.9J/cm^2 were characteristic of amorphous carbon and therefore no intensity ratio could be determined.

The disorder layer thickness remaining after laser irradiation can be determined by comparing the relative intensities of the Raman spectra for the nanosecond and picosecond pulse irradiated samples and by correlating the intensity ratios with RBS measurements of the disordered region of pulsed ruby laser irradiated graphite. A plot of disorder layer thickness versus incident energy density using this method is given in Fig. 3. From Fig. 3 the disorder layer thickness remaining after 20psec pulse irradiation appears to track the 30nsec pulse results well.

For both the nanosecond pulse and picosecond pulse regimes there is a well defined threshold and a region where the disorder layer thickness grows nearly linearly with energy density. For energy densities above 2.0J/cm^2 and 0.5J/cm^2 for the nanosecond pulse and picosecond pulse regimes, respectively, a saturation at $\sim$ 2000Å appears in the disorder layer thickness. The saturation thickness for the picosecond pulses appears smaller than for the nanosecond pulses. This is probably due to differences in the optical properties of graphite at .532μm and 6943Å, reduced thermal transport on a picosecond time scale (i.e. different amounts of vaporisation), and the crudeness of the technique.

The similarity in behavior between nanosecond and picosecond irradiation is verified by examining the irradiated region by transmission electron microscopy. As shown in Fig. 4, the in–plane electron diffraction pattern shows both (00l) rings and (hk0) rings. Patterns of this nature are indicative of a random dispersion of very fine turbostatic graphite grains (no 3–dimensional crystallographic correlations). The grain size in the resolidified material can be determined indirectly by measuring ring widths in electron diffraction patterns or by directly imaging the grain structure. Real space imaging results on samples irradiated in the picosecond regime show randomly oriented turbostatic grains with an a/c aspect ratio of about 2. The grain size on the a-direction is $\sim$10 nm and in the c–direction is $\sim$5 nm. A grain morphology of this nature is consistent with surface energy minimization.

Discussion

From our analysis, the structure of the resolidified material created by both nanosecond pulse and picosecond pulse laser radiation is qualitatively the same. For both cases, the resolidified material is composed of small randomly oriented graphite crystallites which increase in size as the duration of the melt increases. Because of the structural

similarity of the resolidified material, the liquid phases created in both cases must be similar.

The different properties of liquid carbon are based on the fundamental difference in the structure of the liquid necessary for either a liquid metal or insulator phase. A liquid metal model for liquid carbon assumes that the liquid is composed of atomic carbon and that a large fraction of the valence electrons contribute to the electrical transport properties. A liquid insulator model assumes that the liquid is composed of small molecular units where most of the valence electrons will be used in chemical bonding and thus not contribute to electrical transport.

The observation of similar microstrcutures in the resolidified material and the observation of different liquid phases for the two heating regimes may be reconciled by a closer examination of processes occurring during heating. During nanosecond pulse heating there is the expulsion of particles from the surface during the laser pulse which apply pressure to the surface. From a simple conservation of momentum model for the pressure from evolved particles during nanosecond pulsed laser heating[12], the pressure applied during nanosecond pulse laser heating can be as high as 1.5Kbar. From the phase diagram by Ferraz and March, the phase generated by nanosecond pulse laser heating would be a metallic liquid. For the case of picosecond pulse laser heating, the simple conservation of momentum model does not apply because the energy in the pulse will be transferred to the graphite lattice faster than vaporisation can increase the pressure on the surface. The pressure on the surface of the graphite heated in the picosecond regime will hence be lower than for nanosecond pulse heating corresponding to the low pressure region of the Ferraz–March phase diagram.

The similar appearance of the resolidified material may be accounted for by assuming the insulating phase of liquid carbon is composed of small molecular units of carbon. Small molecular units of two to six carbons could form a liquid and upon resolidifying be indistinguishable from the resolidification of an atomic liquid. The properties of the small molecular unit liquid would follow the liquid insulator model since most of the valence electrons would still participate in chemical bonding for molecules as small as C_2.

Conclusions

Similar structures are observed in the resolidified regions of melted graphite created by 20psec pulse 1.06μm Nd:YaG laser irradiation and by 30nsec pulse ruby laser irradiation. Characterization by both Raman spectroscopy and TEM show that in both cases randomly oriented microcrystalline graphite is created. By using Rutherford backscattering data of the resolidified ruby laser melted graphite as a gauge, we can for the first time nondestructively determine the disorder layer thickness for regions irradiated with laser pulses of picosecond duration using Raman spectroscopy. To resolve the controversy in experimentally determined properties of liquid carbon, a more careful examination of the liquid state and solidification processes will be required.

References

[1] T. Venkatesan, D.C. Jacobson, M. Gibson, B.S. Elman, G. Braunstein, G. Dresselhaus and M.S. Dresselhaus, *Phys. Rev. Lett.* 53, 360 1984.

[2] J. Steinbeck, G. Braunstein, M.S. Dresselhaus, T. Venkatesan, and D.C. Jacobson, *J. Appl. Phys.* 58, 4374 1985.

[3] C.Y. Huang, M. Malvezzi, and N. Bloembergen, *Beam-Solid Interactions and Phase Transformations: Proceedings of the Materials Research Society* (Materials Research Society, Pittsburgh) 1985.

[4] A. Ferraz and N.H. March, *Phys. Chem. Liq.* 8, 289 1979.

[5] F.P. Bundy, *J. Chem. Phys.* 38, 618 1963.

[6] M.T. Jones, Report PRC-36 (Nat. Carbon Res. Labs., Ohio) 1958.

[7] T. Venkatesan, B. Wilkens, G. Braunstein, J. Steinbeck, and M.S. Dresselhaus, *Beam-Solid Interactions and Phase Transformations: Proceedings of the Materials Research Society* (Materials Research Society, Pittsburgh) 1985.

[8] N. Bloembergen, *Beam-Solid Interactions and Phase Transformations: Proceedings of the Materials Research Society* (Materials Research Society, Pittsburgh) 1985.

[9] J. Steinbeck, G. Braunstein, M.S. Dresselhaus, T. Venkatesan, D.C. Jacobson, *Energy Beam Solid Interactions and Transient Thermal Processing: Proceedings of the Materials Research Society* (Materials Research Society, Pittsburgh) 1984.

[10] J.S. Speck, J. Steinbeck, G. Braunstein, M.S. Dresselhaus, T.Venkatesan, *Beam-Solid Interactions and Phase Transformations: Proceedings of the Materials Research Society* (Materials Research Society, Pittsburgh) 1985.

[11] F. Tuinstra and J.L. Koenig, *J. Chem. Phys.* 53, 1126 1970.

[12] D.W. Gregg and S.J. Thomas, *J. Appl. Phys.* 37, 2787 1966.

Figure Captions

Figure 1: Phase diagram proposed by Ferraz and March for high temperature and low pressure regime for carbon. The phase transition at ~ 1Kbar was assumed so that the two phases of the liquid may be incorporated in the phase diagram.

Figure 2: Intensity ratio I_{1360}/I_{1582} for laser irradiated graphite as a function laser energy density. for 30nsec ruby laser irradiation (lower abscissa) and 20psec Nd:YaG laser pulses (upper abscissa).

Figure 3: Disorder layer thickness as a function of incident energy density for 20psec 1.06μm Nd:YaG laser pulses and for 30nsec ruby laser pulses. Note the similar behavior including what appears to be saturation near 2000Å.

Figure 4: Selected area electron diffraction pattern from the damaged region of a sample irradiated with 1.7 J cm^{-2} picosecond pulse

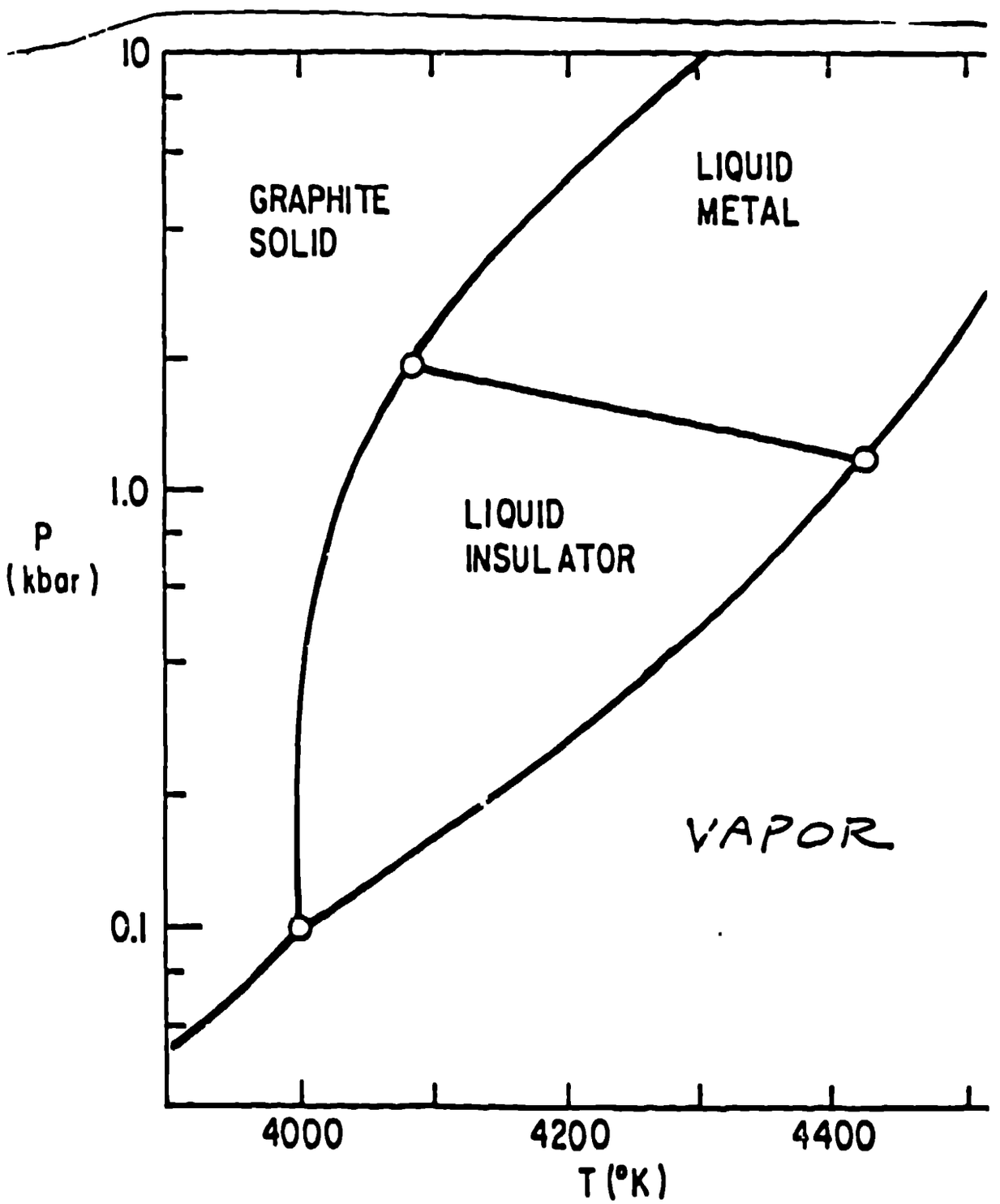
10
1.0
0.1
P
(kbar)
GRAPHITE
SOLID
LIQUID
METAL
LIQUID
INSULATOR
VAPOR
4000
4200
4400
T (°K)

Fig 1

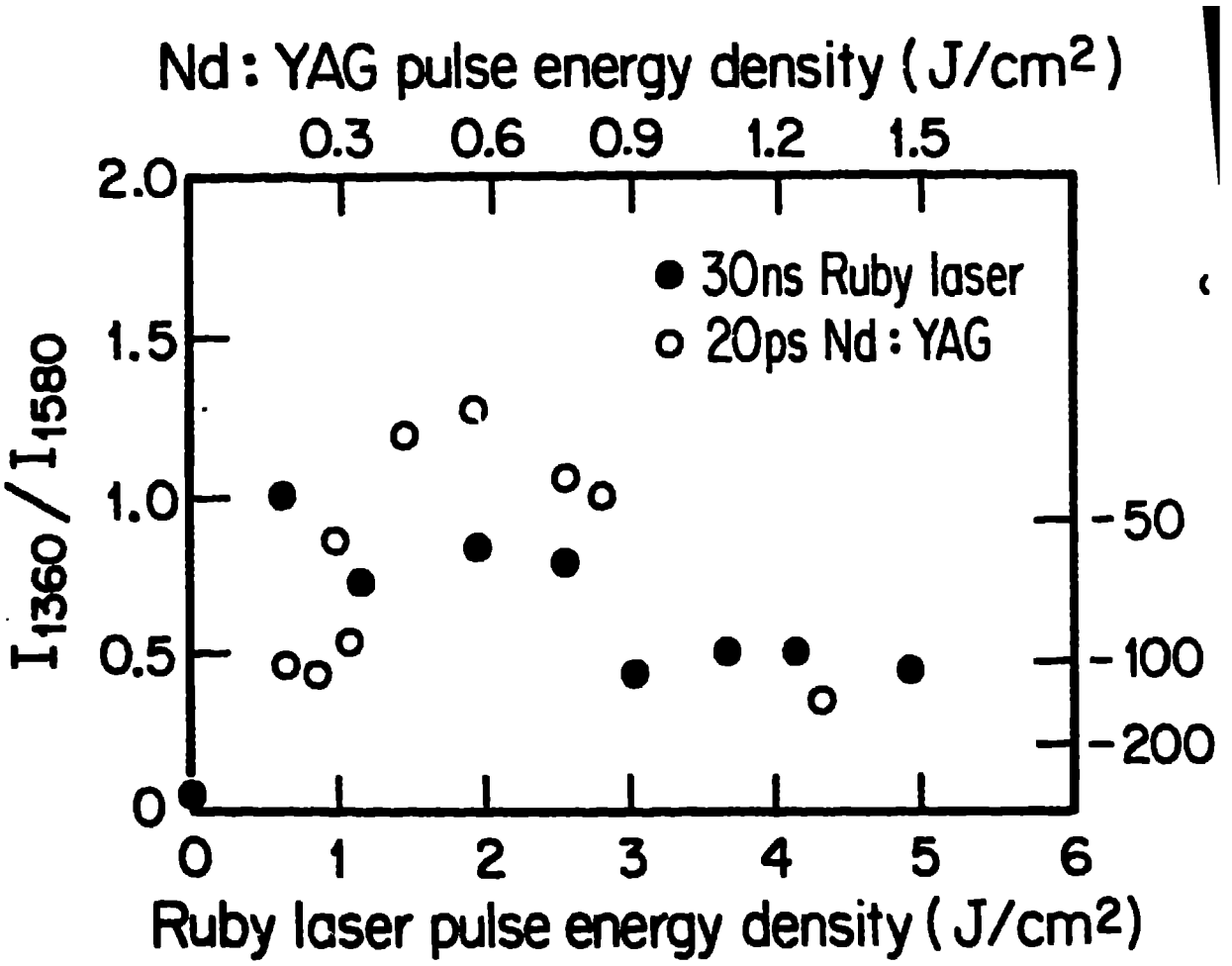

Fig 2

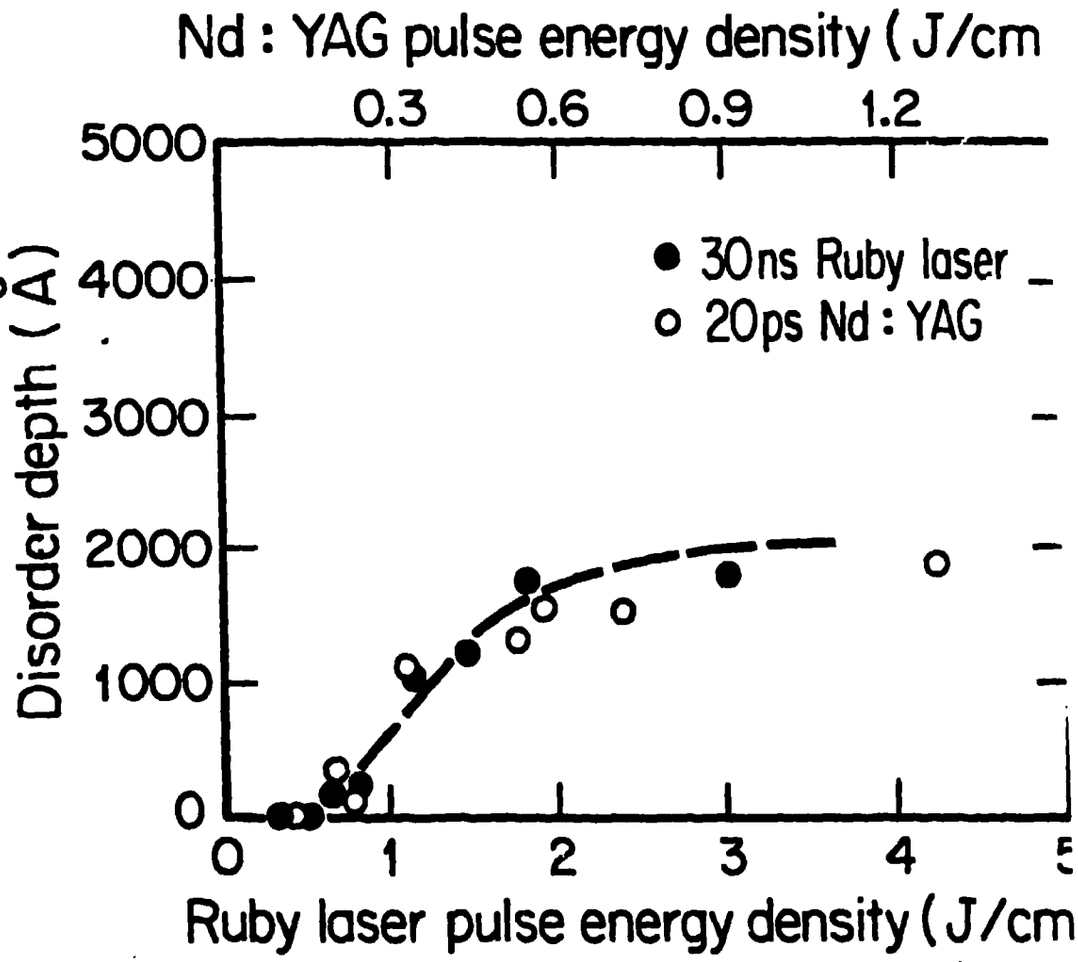
Nd : YAG pulse energy density (J/cm
0.3
0.6
0.9
1.2
5000
4000
3000
2000
1000
0
Disorder depth (Å)
● 30ns Ruby laser
o 20ps Nd : YAG
0
1
2
3
4
Ruby laser pulse energy density (J/cm

Fig 3

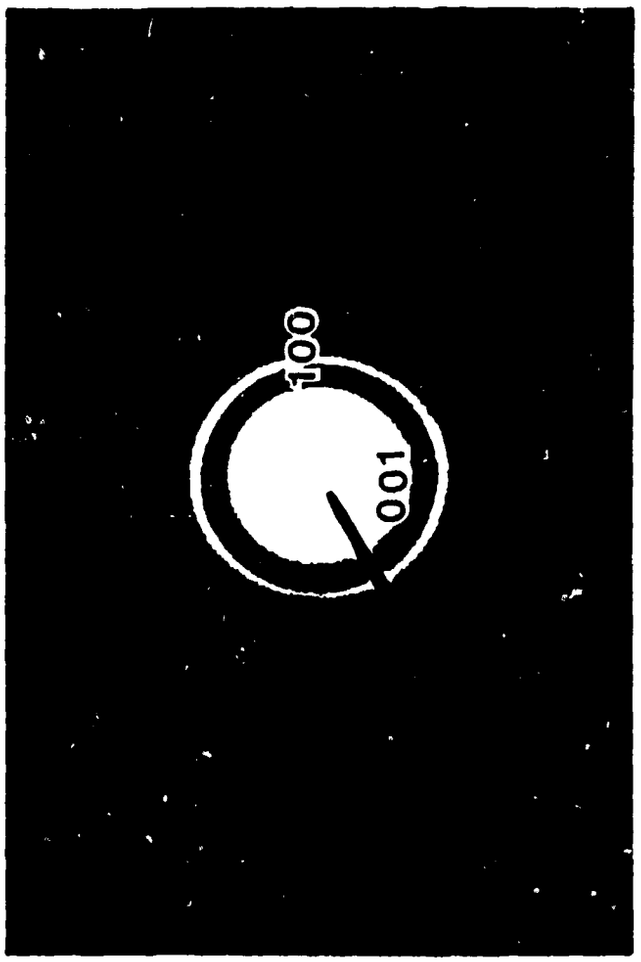

Fig 4